

III. Conclusions

A consistent set of finite-difference equations for the numerical simulation of problems in heat, mass, and/or momentum transfer requires that the finite-difference set possess the same conservation properties as the original differential equations. Not all finite-difference formulations demonstrate this conservation. In particular, the use of a limiting form of the governing equations at the centerline will not result in overall conservation for any finite-difference formulation. Expanding the diffusive term as the sum of two derivatives also leads to errors, regardless of whether or not the centerline of the flow is treated in a limiting fashion.

In order to arrive at a consistent form of the finite-difference equations, the governing differential equation should be integrated over the grid space. This applies to the centerline of the flowfield as well as the exterior points.

Acknowledgment

This work was supported, in part, by the Air Force Office of Scientific Research. The author wishes to thank C.E. Peters and R.P. Rhodes of Aro, Inc, AEDC Division, for suggesting this work.

References

- Roache, P.J., *Computational Fluid Dynamics*, Hermosa Publishers, Albuquerque, N.Mex., 1976, pp. 28ff.
- Fromm, J., "The Time Dependent Flow of an Incompressible Viscous Fluid," *Methods in Computational Physics*, Vol. 3, 1964, pp. 345-382.
- Arakawa, A., "Computational Design for Long-Term Numerical Integration of the Equations of Fluid Motion: Two-Dimensional Incompressible Flow. Part 1," *Journal of Computational Physics*, Vol. 1, Aug. 1966, pp. 119-143.
- Torrance, K.E., "Comparison of Finite-Difference Computations of Natural Convection," *Journal of Research of the National Bureau of Standards (U.S.)*, Vol. 72B, Oct.-Dec., 1968, pp. 281/301.
- Parmentier, E.M. and Torrance, K.E., "Kinematically Consistent Velocity Fields, for Hydrodynamic Calculations in Curvilinear Coordinates," *Journal of Computational Physics*, Vol. 19, Dec. 1975, pp. 404-417.
- Mikatarian, R.R., Kau, C.J., and Pergament, H.S., "A Fast Computer Program for Nonequilibrium Rocket Plume Predictions," Air Force Rocket Propulsion Laboratory, Edwards, Calif., Rept. AFRPL-TR-72-94, Aug., 1972.
- Jensen, D.E. and Wilson, A.S., "Prediction of Rocket Exhaust Flame Properties," *Combustion and Flame*, Vol. 25, Jan. 1975, pp. 43-55.
- Edelman, R.B. and Weilerstein, G., "A Solution of the Inviscid-Viscid Equations with Applications to Bounded and Unbounded Multicomponent Reacting Flows," AIAA Paper 69-83, New York, N.Y., Jan. 1969.

Characteristics of the Split Film Sensor

Colin J. Apelt*

Univeristy of Queensland, Brisbane, Australia

Introduction

A recent innovation in hot-film anemometry has been the development of the split film sensor.¹ The sensor consists of two electrically independent films on a single quartz fiber, as shown in Fig. 1. If each film is operated with a separate anemometer circuit, the total heat transfer from both

Received March 7, 1978; revision received June 19, 1978. Copyright © American Institute of Aeronautics and Astronautics, Inc., 1978. All rights reserved.

Index categories: Viscous Nonboundary-Layer Flows; Sensor Systems.

*Reader, Dept. of Civil Engineering.

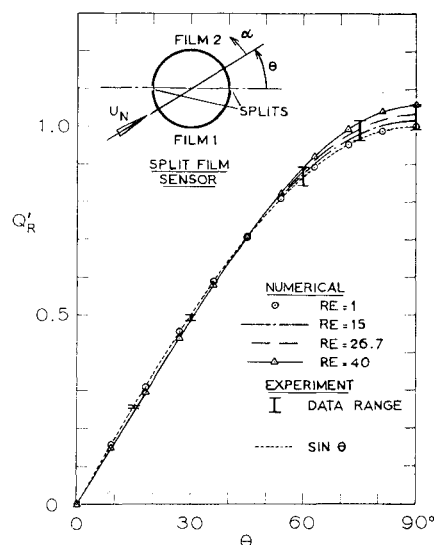


Fig. 1 Difference in heat transfer from the two films of a split film sensor in steady flow; theory and experiment. Values are scaled to make all curves pass through $\sin \theta$ at $\theta = 45$ deg.

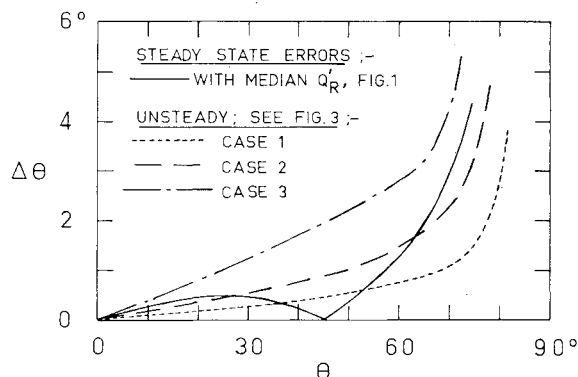


Fig. 2 Errors associated with use of single calibration curve for split film sensor in steady and unsteady flows.

films provides a measure of the magnitude of the velocity vector normal to the axis of the fiber, U_N , while the difference in the heat transfer from the two films provides a measure of the component of the velocity vector perpendicular to the plane of the splits, i.e., $U_N \sin \theta$. The use of the split film sensor has been dependent on data from experimental calibration. This Note presents results obtained from a numerical simulation which shows excellent agreement with experimental data for steady flows. Some effects arising from unsteadiness in the flow are discussed and an analysis of some sources of error in the use of the split film sensor is presented.

Numerical Simulation

The heat transfer from a heated circular cylinder in crossflow was calculated by numerical integration of the Navier-Stokes equation, coupled with the energy equation. The flow was two-dimensional and the fluid was assumed to be incompressible and to have properties which are invariant with temperature.

The heat-transfer characteristics were computed for steady flows at values of Re , the Reynolds number based on cylinder diameter d ranging from 1 to 40 and for a number of unsteady flows. In all calculations the value used for the Prandtl number was 0.7. The details of the numerical simulation are given by Apelt and Ledwich.² The values obtained for the total heat transfer from the cylinder in steady crossflows are in very close agreement with those obtained in a different numerical simulation reported by Dennis et al.³ and are larger than the experimental results of Collis and Williams⁴ by

between 3 and 8%. Such agreement with experimental results is as close as one could realistically expect when the limitations of the mathematical model are taken into account.

Application of Split Film Sensor

The characteristics of a split film sensor were obtained directly from the numerical simulation by separately evaluating the heat transfer from each half of the surface of the cylinder. If Q_1 , Q_2 denote the rate of heat transfer from films 1 and 2, respectively (see Fig. 1), the relationship,

$$Q_1 - Q_2 = f(U_N) \sin \theta \quad (1)$$

is proposed in Ref. 1 as the basis for calibration. This relationship will be strictly correct only if the local rate of heat transfer around the surface of the cylinder, $Q(\alpha)$, varies according to,

$$Q(\alpha) = a - b \cos \alpha \quad (2)$$

where α is measured from the direction of the velocity vector, as shown in Fig. 1, and a , b are functions of Re . In Fig. 1 the results obtained from the numerical simulation for the ratio $(Q_1 - Q_2)/(Q_1 + Q_2)$, denoted by Q_R , are shown for steady flows in the range $1 \leq Re \leq 40$. The values have been scaled in each case to make Q_R equal to $\sin \theta$ at $\theta = 45$ deg, i.e., $Q_R(\theta) = Q_R(\theta) \sin 45 \text{ deg} / Q_R(45 \text{ deg})$. The range of experimental results from Ref. 1, scaled in the same way, are also shown in Fig. 1 and the agreement between these and the numerical results is very good indeed. The experimental data cover an approximate range of Re from 1 to 1000. The curve of $\sin \theta$ is also shown in Fig. 1, and it can be seen that Q_R is very closely approximated by $\sin \theta$ at low values of Re ; the agreement is better than 0.1% at $Re=1$. The differences between Q_R and $\sin \theta$ increase with Re , but it would appear from the experimental results shown in Fig. 1 that the curves of Q_R will lie within the rather small range indicated in Fig. 1 for values of Re between 1 and 1000. Extension of the numerical simulation to larger values of Re to check this is desirable, even though this will be a substantial task since periodic vortex shedding must be allowed for when $Re > 40$.

It would be very convenient if a single calibration curve could be used for all values of Re and, indeed, the median curve of Q_R could be used for this purpose with sufficient accuracy for many applications. A measure of the accuracy of such a procedure is given by the associated error in the determination of the angle θ , denoted by $\Delta\theta$. The maximum errors resulting from use of the median curve of Q_R as the calibration at all values of Re are shown in Fig. 2. It can be seen that $\Delta\theta$ has a magnitude less than 0.5 deg for $\theta < 52$ deg. The error grows rapidly with larger values of θ , an inevitable consequence of scaling Q_R so as to achieve no error at $\theta = 45$ deg. Better accuracy could be achieved, of course, if a more complex relationship than that indicated by Eq. (1) were used, and if the dependence on Re were allowed for. Such a relationship could be formulated when results have been obtained from numerical simulations at larger values of Re .

Effects of Unsteadiness

All of the preceding discussion has related to the response of the split film sensor to a steady velocity vector or to the temporal mean velocity vector in turbulent flow. When the sensor is used in turbulent flow to indicate, for example, the direction of the instantaneous velocity vector there is introduced a new source of error in that the distribution of heat transfer around the surface of the cylinder in a steady velocity field is not exactly the same as that in an unsteady velocity field at the same (instantaneous) value of Re . This is illustrated in Fig. 3 where the curves of Q_R obtained in the numerical simulation for three unsteady flows are compared with the appropriate steady-state curves. For the first case, a sinusoidal fluctuation in velocity of amplitude of 10% and

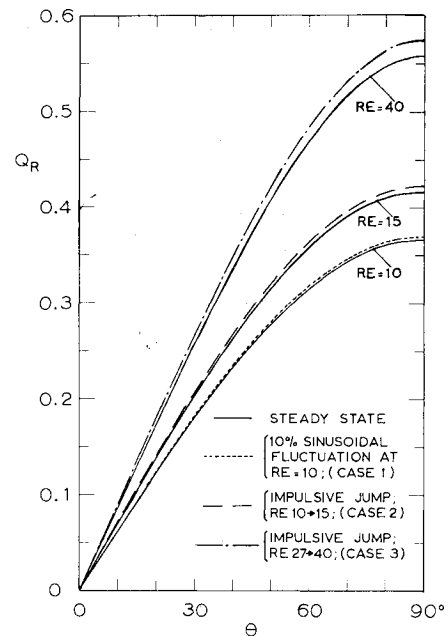


Fig. 3 Effects of unsteadiness of flow on heat-transfer characteristics of split film sensor.

frequency $0.14 U_N/d$ Hz was applied to a mean flow at $Re=10$. The other two cases involved impulsive increases in velocity of 50%. The curves shown for cases 2 and 3 in Fig. 3 correspond to conditions at times of $0.83 d/U_N$ s and $1.05 d/U_N$ s after the impulsive increase in velocity, respectively. The time constant, i.e., the time taken for the response to reach 0.63 of the increment to the final value, had the values $1.16 d/U_N$ in case 2 and $0.81 d/U_N$ in case 3. In all three cases the cylinder was treated as having no thermal inertia.

In application to unsteady flow, a steady-state calibration must be used and, consequently, the extra errors arising from unsteadiness will be essentially unaffected by the type of steady-state calibration used. To indicate the order of magnitude of the extra errors arising from unsteadiness in turbulent flow the errors associated with the three specific cases of Fig. 3 have been shown in Fig. 2. It can be seen that the extra errors arising from unsteadiness can be substantial. The two cases of impulsive velocity changes give conditions which are unlikely to be met in normal experimentation. However, the case of periodic fluctuation in velocity results in extra errors which are comparable to those associated with the steady-state calibration curves discussed in preceding sections. In fact, it can be inferred from Fig. 2 that the accuracy of results obtained with a split film sensor in turbulent flow will deteriorate seriously if the angle between the mean velocity vector and the plane of the split exceeds 45 deg, or if the turbulence intensity is very large.

Acknowledgment

Financial support received from the Australian Research Grants Committee is gratefully acknowledged.

References

- 1 TSI Split Film Sensor. Calibration and Applications, Thermo-Systems Inc., Tech. Bull. TB20.
- 2 Apelt, C.J. and Ledwith, M.A., "Transient and Unsteady Cross-Flows Past a Heated Circular Cylinder in the Range $1 \leq Re \leq 40$," submitted to *Journal of Fluid Mechanics*, 1977.
- 3 Dennis S.C.R., Hudson, J.D., and Smith, N., "Steady Laminar Forced Convection from a Circular Cylinder of Low Reynolds Numbers," *The Physics of Fluids*, Vol. May 11, 1968, pp. 933-942.
- 4 Collis, D.C. and Williams, M.J., "Two-Dimensional Convection from Heated Wires at Low Reynolds Numbers," *Journal of Fluid Mechanics*, Vol. 6, Oct. 1959, pp. 357-384.